Original Article

Pediatric Craniospinal Irradiation – The implementation and Use of Normal Tissue Complication Probability in Comparing Photon versus Proton Planning

S. Balasubramanian[1,2], M. K. Shobana[2]

[1]Department of Radiation Oncology, Max Super Specialty Hospital, Ghaziabad, Uttar Pradesh, [2]Department of Physics, School of Advanced Sciences, Vellore Institute of Technology, Vellore, Tamil Nadu, India

Abstract

Purpose: The preferred radiotherapy treatment for medulloblastoma is craniospinal irradiation (CSI). With the aim of developing the potential to reduce normal tissue dose and associated post-treatment complications with photon and proton radiotherapy techniques for CSI. This report aims to carefully compare and rank treatment planning and dosimetric outcomes for pediatric medulloblastoma patients using normal tissue complication probability (NTCP) formalism between photon (three-dimensional conformal radiotherapy, intensity-modulated radiotherapy [IMRT], volumetric-modulated arc therapy [VMAT], and HT) and proton CSI. **Methods and Materials:** The treatment data of eight pediatric patients who typically received CSI treatment were used in this study. The patients were 7 years of age on average, with ages ranging from 3 to 11 years. A prescription dose of 3600 cGy was delivered in 20 fractions by the established planning methods. The Niemierko's and Lyman–Kutcher–Burman models were followed to carefully estimate NTCP and compare different treatment plans. **Results:** The NTCP of VMAT plans in upper and middle thoracic volumes was relatively high compared to helical tomotherapy (HT) and pencil beam scanning (PBS) (all $P < 0.05$). PBS rather than IMRT and VMAT in the middle thoracic region ($P < 0.06$) could significantly reduce the NTCP of the heart. PBS significantly reduced NTCP of the lungs and liver (all $P < 0.05$). **Conclusion:** The NTCP and tumor control probability (TCP) model-based plan ranking along with dosimetric indices will help the clinical practitioner or medical physicists to choose the best treatment plan for each patient based on their anatomical or clinical challenges.

Keywords: Craniospinal irradiation, normal tissue complication probability, radiobiological model, radiotherapy, tumor control probability

Received on: 03-06-2021 **Review completed on: 12-08-2021** **Accepted on: 13-08-2021** **Published on: 20-11-2021**

Introduction

Central nervous system (CNS) tumors are the leading malignant brain tumor in children[1] and an uncommon brain tumor in adults. It begins inside the cerebellum, which controls cognitive abilities. Nearly 20% of all primary CNS tumors are medulloblastoma, which occurs among kids with an uttermost incidence between 5 and 9 years. Medulloblastoma is also one of the most radiosensitive childhood brain tumors; hence, radiation therapy (RT) is undoubtedly considered the treatment of choice.[2]

When craniospinal irradiation (CSI) is specified, the treatment volume encompasses to include the entire CNS subarachnoid space. The lateral cranial fields as well as one or more posterior spine fields were routinely used to treat this volume. To encompass the thecal sac, the inferior border for the spinal field extends below S2 (sacral spine). However, carefully balancing the cranial and spinal fields needs intensive technical preparation to achieve a homogeneous dose distribution and it depends on several factors, including the modality chosen for the treatment of the spinal field.

The treatment of CSI contains a complex anatomical structure that requires complex treatment planning, which additionally

Access this article online

Quick Response Code:

Website: www.jmp.org.in

DOI: 10.4103/jmp.jmp_75_21

Address for correspondence: Dr. M. K. Shobana, School of Advanced Sciences, Vellore Institute of Technology, Vellore - 632 014, Tamil Nadu, India.
E-mail: shobana.mk@vit.ac.in

How to cite this article: Balasubramanian S, Shobana MK. Pediatric craniospinal irradiation – The implementation and use of normal tissue complication probability in comparing photon versus proton planning. J Med Phys 2021;46:244-52.

requires several isocenters need to be set and many fields to be matched to achieve agreeable plan. Like three-dimensional conformal radiotherapy (3DCRT), volumetric-modulated arc therapy (VMAT), intensity-modulated radiotherapy (IMRT), helical tomotherapy (HT), and proton beam scanning (PBS), several radiotherapy techniques are also used for CSI treatment.

The main objective of radiotherapy is to achieve a high local tumor control probability (TCP) and at the same time to reduce the normal tissue complication probability (NTCP). The goal of this study is to compute and rank treatment plans in CSI for pediatric patients using the dosimetric indexes such as prescription dose to the planning target volume (PTV), homogeneity index (HI), conformity index (CI), target coverage index, and quality factor. Furthermore, radiobiological indexes such as equivalent uniform dose (EUD)-based TCP and NTCP are calculated and used for justification in 3DCRT, IMRT, VMAT, HT, and PBS. The model-based probability NTCP was used to choose the best treatment plan.

The evaluation of the radiotherapy treatment plan is based on a definite assessment of the TCP and NTCP resulting from the dose distribution. The possible application of radiobiological modeling to radiotherapy is the rating of treatment plans by an explicit determination of TCP and NTCP values.[3-5] Furthermore, this paper outlines dose–response relationship for early and late radiation responses as well as tumor control. We have developed an in-house software tool with Matlab (Mathworks) to evaluate the TCP and NTCP arising from the differential dose-volume histograms (dDVHs). The program was developed to integrate related present knowledge of the radiobiological model and assists in the potential estimation of competing treatment plans by enabling evaluation and comparison of different model predictions.[6-10]

Materials and Methods

Patient selection and contouring

The treatment data of eight pediatric patients who received CSI treatment are used in this study. The patients were 7 years of age on average, with ages ranging from 3 to 11 years with four female and four male pediatric patients who were presented for this study. CT images are transferred to a Monaco® treatment planning system (Elekta Medical Systems, Stockholm) where the target volumes (brain and spinal cavity) and organs at risk (OARs) were defined as per RTOG (0529 and 0539) guidelines. The clinical target volume (CTV) brain included the whole brain and the meninges. CTV spinal cavity included C1 through S2. The spinal cavity and brain PTVs were created by evenly growing with volumetric margins of 10 mm and 5 mm, respectively, in all directions from the corresponding CTVs. Heart, lungs, liver, mandible, stomach, bowel, external genitalia, kidneys, and optical structures such as eyes, lens, optic nerves, and optic chiasm were the OARs delineated and used for comparison.

Treatment planning

For each patient, five independent treatment plans were generated, including 3DCRT, VMAT, IMRT, HT, and PBS. An aggregate dose of 3600 cGy was planned in 20 fractions[11,12] consistent with the defined planning protocol. The Monaco® treatment planning station was used to generate the 3DCRT, VMAT, and IMRT plans. Monte Carlo (MC)-based calculation engine was used for the dose calculation for all the three plans. The precision planning station (Accuray Inc, WI, USA) was used to generate the HT plans with GPU-based VoLO dose calculation and optimization algorithm. Raystation planning system (RaySearch Laboratories, Sweden) was used to generate the proton pencil beam scanning (PBS) plan; GPU Monte carlo dose calculation engine for optimization and final dose calculation was used. All the plans were calculated with 2-mm grid resolution.

For the conventional 3DCRT, two parallel opposed lateral fields are used for the brain PTV and 1–2 posterior fields were used for spine PTV. To prevent the divergence of the beam into the spine fields, the couch is shifted and also the collimator is additionally rotated to match the divergence of the spine field. Cranial fields used a source to axis distance (SAD) setup, while the spine fields used source to surface distance (SSD) setup. If necessary, the feathering technique was accustomed to achieve homogeneous dose distribution.[13]

VMAT and IMRT plans were developed using a bias dose planning method to prevent junction overlap and to achieve a uniform dose without feathering.[14] The VMAT plans consisted of two partial arcs rotated in opposite directions to cover the superior part of the PTV. The fan beam was used to develop the HT plans with 2.5-mm thickness, a modulation factor of three, and a pitch of 0.3. The optimization was continued until the further reduction in OAR dose is possible without compromising coverage or increasing hot spots. A vertebral-body-sparing technique was used in the PBT plan.[15] The plans were normalized to 95% of the prescription dose to cover 95% of the PTV. Figure 1 shows the dose distribution comparison of all the various plans 3DCRT, IMRT, VMAT, HT, and PBS, respectively.

Treatment plan evaluation

A diverse radiotherapy modality treatment plans require grading and comparing with the calculation of DVH and radiation outcome. The target volume and relevant QARs of the plans were quantitatively evaluated with the DVH analysis. The following indices are used in this study.

Coverage index (CI):

$$CI = \frac{D_{min}}{PD}$$

D_{min} is the minimum dose encompassing the PTV and PD is the prescribed dose to the PTV.

Conformity Index for the target volume (CI_{TV}):

$$CI_{PTV} = \frac{Volume\ receiving\ 95\%\ of\ PD}{PTV\ Volume}$$

Dose HI (DHI): DHI is used to quantify the hot spots surrounding and inside the PTV, as:

$$DHI = \frac{D_{max}}{PD}$$

D_{max} is the maximum dose in the PTV and PD is the prescribed dose to the PTV.

Modified dose HI (MHI) is defined as:

$$MHI = \frac{D_{95}}{D_5}$$

The dose to 95% of the PTV is D_{95} and the dose to 5% of the PTV is D_5.

Normal tissue complication probability calculation models

Lyman–Kutcher–Burman normal tissue complication probability model

A mathematically similar but simpler formulation of the Lyman–Kutcher–Burman (LKB) model has been proposed. Various researchers including Burman *et al*. fit tolerance dose data into a phenomenological NTCP model proposed by Lyman, Kutcher, and Burman later developed a way for dose volume histogram (DVH) reduction that can take heterogeneous dose distributions into account.[16-18] The combined formalism is denoted as the LKB model.

$$NTCP = \frac{1}{\sqrt{2\pi}} \int_{-\infty}^{t} e^{-\frac{x2}{2}} dx$$

$$t = \frac{D_{eff} - TD_{50}}{m \times TD_{50}}$$

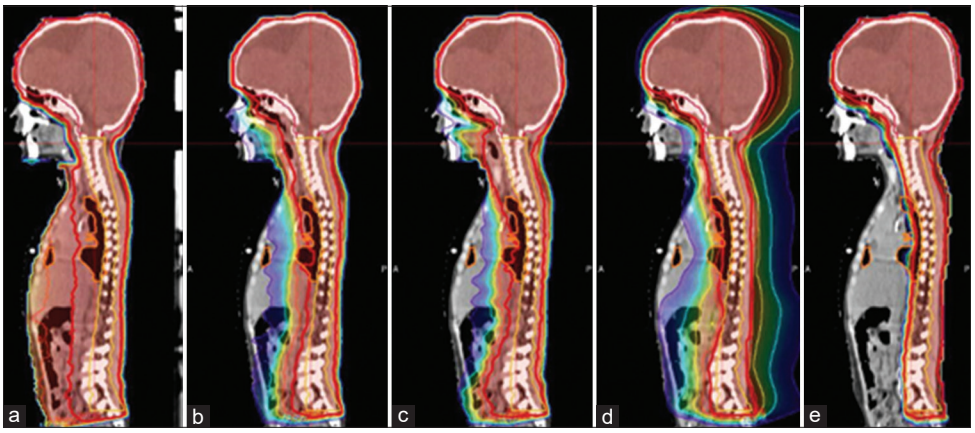

Figure 1: Dose coverage for a single patient for the plan three-dimensional conformal radiotherapy (a), intensity-modulated radiotherapy (b), volumetric-modulated arc therapy (c), HT (d), and pencil beam scanning (e)

Table 1: Set of parameters used for Lyman-Kutcher-Burman and Niemierko's equivalent uniform dose-based normal tissue complication probability calculation[19-23]

Organ	A	γ50	TD50	*n*	*m*	α/β	Endpoint
Brain	5	3	60	0.25	0.15	2.1	Necrosis
Brainstem	7	3	65	0.16	0.14	3	Necrosis
Colon	6	4	55	0.17	0.11	3	Obstruction/perforation
Esophagus	19	4	68	0.06	0.11	3	Perforation
Heart	3	3	48	0.35	0.1	3	Pericarditis
Kidney	1	3	28	0.7	0.1	3-3.5	Nephritis
Lens	3	1	18	0.3	0.27	1.2	Cataract
Liver	3	3	40	0.32	0.15	1.5	Liver failure
Lung (R and L)	1	2	24.5	0.87	0.18	3*	Pneumonitis
Optic nerve	25	3	65	0.25	0.14	3-3.5	Blindness
Optic chiasm	25	3	65	0.25	0.14	3	Blindness
Retina	15	2	65	0.2	0.19	3	Blindness
Stomach	6	4	59	0.09	0.3	7-10	Gastric bleeding
Mandible	14	4	72	0.07	0.1	3-3.5	Limitation of the joint function

*α/β value assumed as 3

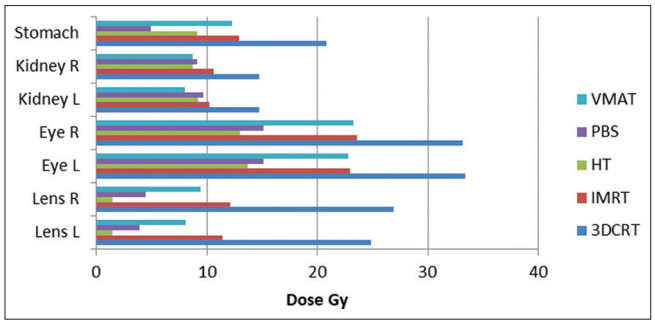

Figure 2: Equivalent uniform dose calculated for organ at risk for three-dimensional conformal radiotherapy, intensity-modulated radiotherapy, volumetric-modulated arc therapy, HT, and pencil beam scanning

$$Deff = \left(\sum_i V_i D_i^{\frac{1}{n}} \right)^n$$

where TD_{50} is the tolerance dose for the organ uniformly irradiated that would lead to a complication probability of 50%. D_{eff} is the dose that, if given uniformly to the whole volume, will result in the same NTCP as the original inhomogeneous distribution of the dose, D_i is the dose given to each bin in the dDVH, V_i is the volume in a specific dose bin *i, m* is the dimensionless parameter to determine the slope of the complication probability versus dose curve, and *n* is the volume dependence of the probability of complication. The endpoints are addressed by Emami *et al*.[19] The corresponding sets of parameters for TD_{50}, endpoints, m, and n are shown in Table 1.

In the LKB model, biological dose correction is also considered. This is significant because the heterogeneity of the dose in normal tissues can cause biological effects due to the different fraction sizes as well as the overall dose. Furthermore, if other than 2 Gy per fraction are used, the nonadjusted DVH may not reflect the biological effect. Each dose bin could be accounted for by estimating the equivalent dose of 2 Gy per fraction (EQD_2) as follows:

$$EQD_2 = D_i \frac{\left(\frac{\alpha}{\beta} + \frac{D_i}{n_f} \right)}{\left(\frac{\alpha}{\beta} + 2 \right)}$$

where D_i is the total dose received by the bin, n_f is the total number of fractions, and D_i/n_f is the dose per fraction size received by the dose bin. α/β are the linear-quadratic (LQ) model parameters for the specific organ being typically exposed. This adjusted dDVH can then be applied to the LKB equations as described above.

Niemierko's equivalent uniform dose model

Equivalent uniform dose

The EUD is defined as the absorbed dose that, if given homogeneously to the tumor or normal tissue, will have the equivalent biological effect as the actual nonhomogeneous irradiation. It is described as follows:

$$EUD = \left(\sum_{i=1} V_i \; EQD_i^a \right)^{1/a}$$

where EQD_i is dose delivered to a subvolume V_i, and *a* is a unitless model parameter that is specific to the normal structure or tumor of interest.

According to Niemierko's model, the following equations were used to determine the dose of two grays in each fraction, TCP and NTCP.

$$EQD_i = D_i \frac{\left(\frac{\alpha}{\beta} + \frac{D_i}{n_f} \right)}{\left(\frac{\alpha}{\beta} + 2 \right)}$$

where D_i is the total dose received by the bin, n_f is the total number of fractions, and D_i/n_f is the dose per fraction size received by the dose bin. α/β are the LQ model parameters for the specific organ being typically exposed.

The TCP is calculated from the following formula:

$$TCP = \frac{1}{1 + \left(\frac{TCD_{50}}{EUD} \right)^{4\gamma_{50}}}$$

The NTCP is calculated from the following formula:

$$NTCP = \frac{1}{1 + \left(\frac{TD_{50}}{EUD} \right)^{4\gamma_{50}}}$$

The γ_{50} is a unitless model parameter that describes the slope of the dose–response curve. TCD_{50} is the tumour dose to control 50% of the tumour when the target is homogeneously irradiated and TD_{50} is the tolerance dose for a 50% complication rate at a specific time interval when the entire organ of interests were homogeneously irradiated.[20-23] The set of parameters used for Niemierko's EUD model calculations is succinctly summarized in Table 1.

Results

The target coverage at 3600 cGy delivered by the 3DCRT plans was determined by 95% (±1%) to provide a clear-cut evaluation between IMRT, VMAT, HT, PBS, and 3DCRT techniques. To meet this target coverage, competing plans have rescaled. The mean value and standard deviation values for various dosimetric parameters for the PTV and OARs were analyzed in Tables 2 and 3. The percentage of kidney receiving 30% of the prescription dose was also statistically substantially reduced with tomotherapy [Figure 2]. The lowest lens dose was observed in the PBS technique, but all methods were within tolerance limits. An extensive reduction in maximum dose to PTV was achieved by increased conformity

Table 2: Mean dose for organ at risk for patient A

Target (patient A)	Parameter	3DCRT	IMRT	VMAT	HT	PBS
Normal tissue	$V_{95\%}$ (%)	0.21	0.26	0.38	0.20	0.16
Lens	Mean (Gy)	7.60	6.01	6.81	5.99	5.08
Thyroid	Mean (Gy)	8.11	7.13	6.52	5.86	6.17
Lung	Mean (Gy)	6.34	6.47	7.24	6.94	5.84
Heart	Mean (Gy)	4.63	4.19	4.25	3.23	4.03
Liver	Mean (Gy)	3.94	4.10	4.08	3.84	3.19
Spleen	Mean (Gy)	4.35	5.12	5.49	4.25	4.02
Kidney	Mean (Gy)	8.37	7.24	7.20	7.32	7.11
Esophagus	Mean (Gy)	11.08	9.06	8.12	6.51	4.73
Left optic nerve	Mean (Gy)	21.19	22.04	21.15	20.18	20.03
Right optic nerve	Mean (Gy)	20.40	18.27	17.36	16.79	16.59

3DCRT: Three-dimensional conformal radiotherapy, IMRT: Intensity-modulated radiotherapy, VMAT: Volumetric arc therapy, HT: Helical tomotherapy, PBS: Proton beam scanning

Table 3: Evaluation indices with standard deviation of planning target volume brain and spinal cavity

	PTV_brain					PTV_spinal cavity				
	3DCRT	IMRT	VMAT	HT	PBS	3DCRT	IMRT	VMAT	HT	PBS
Dmax (SD)	36.6 (0.4)	37.2 (1.2)	37.8 (1.7)	38.1 (0.4)	38.7 (1.2)	37.9 (0.9)	38.5 (1.2)	38.9 (1.2)	37.1 (0.9)	38.7 (1.6)
Dmin (SD)	20.5 (7.1)	24.1 (2.9)	25.5 (2.0)	26.3 (1.5)	29.8 (5.4)	26.9 (9.1)	27.4 (1.8)	28.4 (1.8)	24.7 (1.1)	30.8 (2.4)
Dmean (SD)	36.4 (0.3)	35.1 (0.6)	36.3 (0.8)	35.7 (3.5)	36.5 (0.6)	38.4 (1.3)	36.2 (1.4)	36.9 (1.4)	36.8 (1.2)	37.5 (1.0)
V95% (SD)	98.3 (0.6)	97.6 (0.5)	97.0 (0.5)	99.3 (2.4)	99.3 (1.4)	99.3 (3.3)	97.1 (0.9)	97.8 (0.9)	98.3 (1.4)	98.3 (0.3)
DHI (SD)	0.80 (0.0)	0.88 (0.0)	0.94 (0.0)	0.99 (0.0)	0.97 (0.0)	0.79 (0.0)	0.92 (0.0)	0.94 (0.0)	0.98 (0.0)	0.94 (0.0)
CI (SD)	0.90 (0.2)	0.89 (0.0)	0.91 (0.0)	0.95 (0.0)	0.94 (0.0)	0.90 (0.4)	0.93 (0.0)	0.94 (0.0)	0.96 (0.0)	0.94 (0.0)

3DCRT: Three-dimensional conformal radiotherapy, IMRT: Intensity-modulated radiotherapy, VMAT: Volumetric arc therapy, HT: Helical tomotherapy, PBS: Proton beam scanning, PTV: Planning target volume, SD: Standard deviation, DHI: Dose homogeneity index, CI: Conformity index

Table 4: Normal tissue complication probability for optic nerve left for Niemierko's equivalent uniform dose method

	NTCP_niem/optic nerve left				
Patient	3D	IMRT	HT	PBS	VMAT
1	0.06459469	0.02571542	0.032123025	0.0219478	0.057622930
2	0.11413804	0.02602748	0.009011407	0.0070571	0.070100971
3	0.11235983	0.05655873	0.032300464	0.0061253	0.056014464
4	0.10151674	0.01055849	0.000640399	0.0120379	0.125206737
5	0.12949373	0.02153305	0.025962562	0.0172667	0.120950500
6	0.09234197	0.01724776	0.04102101	0.0254175	0.081356098
7	0.07654791	0.01994038	0.026387868	0.0249434	0.026107633
8	0.10169208	0.02050167	0.006632658	0.0247497	0.058451718

IMRT: Intensity-modulated radiotherapy, VMAT: Volumetric arc therapy, HT: Helical tomotherapy, PBS: Proton beam scanning, NTCP: Normal tissue complication probability

of the techniques such as IMRT and VMAT. The surprising difference is that VMAT gives a lower radiation dose to a larger volume of OAR. This was observed in other studies with VMAT triggered by the low radiation dose bath as a result of continuous delivery of the dose over a wide range of gantry angles.

The averaged mean dose of all eight patients for different organs calculated using the bootstrap method is shown in Table 2 (95% confidence interval). The mean dose in the PBS plan was significantly lower than all other plans for organs, which are farther away from target volumes such as the heart, esophagus, liver, and bowel. 3DCRT standard plans had the highest mean doses since the volume of normal tissue received by the prescribed dose was higher, approximately 50%.

Tomotherapy generated more superior CI and HI than VMAT and IMRT for PTV brain (HI, $P < 0.001$; CI, $P = 0.004$). However, PTV spine HI in the PBS plan had acceptable dose homogeneity ($P = 0.001$). D mean of PTV brain was significantly different, together with D98 of PTV spine ($P < 0.05$) in HT, VMAT, IMRT, and PBS [Table 3].

Although two different methods including Niemierko's model and LKB model were used to compute NTCP, the similar

Table 5: Normal tissue complication probability for optic nerve right for Lyman-Kutcher-Burman method

	NTCP_LKB/optic nerve right				
Patient	**3D**	**IMRT**	**HT**	**PBS**	**VMAT**
1	0.05381226	0.01036990	0.01000828	0.04965759	0.02502120
2	0.11411970	0.01382660	0.00153152	0.04059398	0.03218160
3	0.10373518	0.00752172	0.00933767	0.05032167	0.03256377
4	0.09112276	0.02374548	5.7007E-05	0.05122253	0.01804040
5	0.12126287	0.00514249	0.00047995	0.04541476	0.00794657
6	0.07948107	0.01200963	0.00225403	0.05254994	0.03997440
7	0.06305404	0.00886599	0.02994166	0.05820718	0.03106334
8	0.07878493	0.00772817	3.7903E-05	0.05956650	0.00993672

NTCP: Normal tissue complication probability, IMRT: Intensity-modulated radiotherapy, VMAT: Volumetric arc therapy, HT: Helical tomotherapy, PBS: Proton beam scanning

Table 6: D_{eff} of left eye for Lyman-Kutcher-Burman method

	Deff/left eye				
Patient	**3D**	**IMRT**	**HT**	**PBS**	**VMAT**
1	34.5514447	21.0785849	12.3741695	14.6990508	21.56205443
2	32.9117037	22.9930320	15.7010263	14.9755675	22.86697161
3	34.8807373	27.4811487	12.3986378	15.4115996	25.76534440
4	34.3688044	21.1590613	10.5006192	14.8014158	21.06589910
5	34.0041074	23.2345864	16.8443471	14.7083697	22.80678020
6	32.7686694	20.2581433	9.49853366	14.7429171	22.38209819
7	33.0005569	22.7507805	19.0932519	14.7859149	22.07190818
8	30.6970930	24.5646955	13.2767078	16.8203700	23.93408923
8	16.7565565	6.48664324	4.93845574	2.54408554	6.699462858

IMRT: Intensity-modulated radiotherapy, VMAT: Volumetric arc therapy, HT: Helical tomotherapy, PBS: Proton beam scanning

Table 7: Equivalent uniform dose of heart for Niemierko's equivalent uniform dose method

	EUD/heart				
Patient	**3D**	**IMRT**	**HT**	**PBS**	**VMAT**
1	22.3854885	9.39319554	8.523711934	0.5236425	11.77227773
2	22.9246091	8.89878483	6.157979160	0.5895947	10.94543398
3	25.0783815	10.0802663	8.551845841	0.7024990	11.48415693
4	23.4896337	7.15589484	4.823317791	0.6015577	8.641169421
5	22.5964097	6.49450708	7.027654168	0.1085553	7.673569563
6	21.7410449	9.82843956	5.844027684	0.1494359	11.05120520
7	23.5720482	7.77743002	6.183950099	0.5893934	10.33514946
8	24.4268448	6.44610008	5.224331662	0.8970121	6.716136078

EUD: Equivalent uniform dose, IMRT: Intensity-modulated radiotherapy, VMAT: Volumetric arc therapy, HT: Helical tomotherapy, PBS: Proton beam scanning

results were observed. PBS returned better quality of NTCP compared to IMRT and VMAT ($P < 0.02$). The VMAT NTCP was relatively high compared to HT and PBS (all $P < 0.05$) for upper and middle thoracic volumes. However, the better NTCP value is shown by the VMAT plan for the lower thoracic region followed by HT, and 3DCRT plan had the lowest outcome. Figures 3 and 4 show the NTCP variations of 3DCRT, IMRT, VMAT, HT and PBS plans for esophagus and mandible calculated by EUD and LKB methods respectively. Furthermore, this study establishes that the PBS plan shows a significant reduction in heart mean dose compared to IMRT and VMAT in the mid-thoracic area ($P < 0.06$). Furthermore, the PBS plan significantly reduced NTCP of the lungs and liver doses (all $P < 0.05$). Tables 4 and 5 list the NTCP statistics for the left and right optic nerves. Tables 6 and 7 shows the Deff and EUD values of the left eye and heart for 3DCRT, IMRT, HT, PBS and VMAT plans respectively.

Discussion

The IMRT and VMAT techniques are advancements in CSI treatment compared to the 3DCRT technique; none of these approaches enables to omit field matching and junction shift,

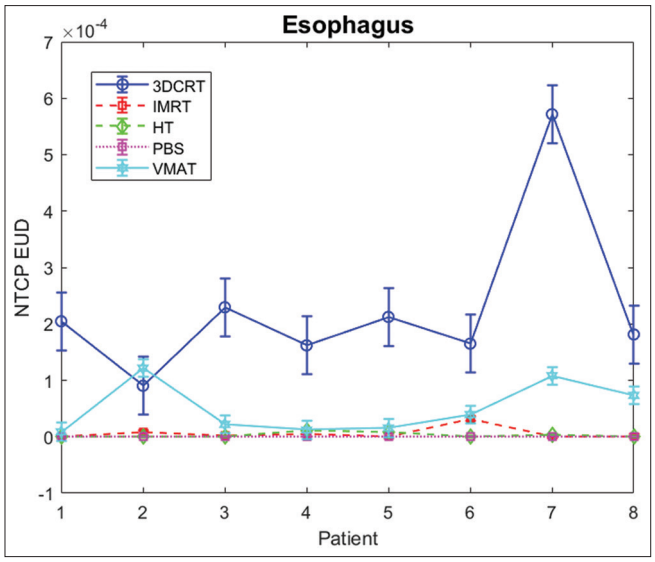

Figure 3: Normal tissue complication probability calculated for esophagus using equivalent uniform dose method for three-dimensional conformal radiotherapy, intensity-modulated radiotherapy, volumetric-modulated arc therapy, HT, and pencil beam scanning

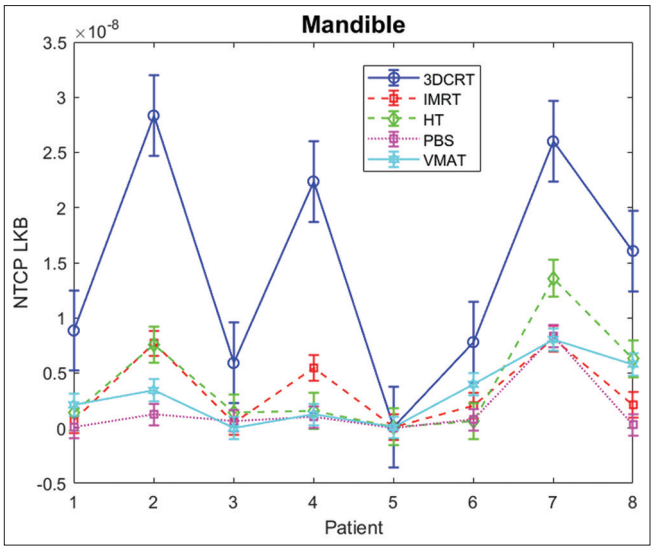

Figure 4: Normal tissue complication probability calculated for mandible using Lyman–Kutcher–Burman method for three-dimensional conformal radiotherapy, intensity-modulated radiotherapy, volumetric-modulated arc therapy, HT, and pencil beam scanning

which may cause unplanned underdose or overdose in the spinal cord if the minimal setup error occurs during the patient positioning and thus can contribute to disease recurrence or lead to severe side effects. The smooth, helical delivery of the intensity-modulated fan-beam, which allows the treatment of extended volumes in the cranio-caudal direction without the need for junction, is a novel advancement for the CSI treatment.[24]

During past decades, we have observed the evolution of novel and advanced treatment techniques such as tomotherapy and PBS.[25,26] In addition, advances in biology and functional imaging in cancer care with the advancement in computer technology have had a significant impact on developing good plans. It is assertively founded by this study that the comparison of only dosimetric metrics is not sufficient for the evaluation of similar and complex plans. Because in some cases, large dosimetric differences do not result in substantial TCP and NTCP differences between two treatment plans and vice versa.

Numerous studies have investigated the LQ model of cell killing to rank treatment plans.[27-30] The correlation between NTCP and EUD examined in this study with parameters obtained from DVH is to provide a prompt and new way to compare treatment plans. The DVH parameters were generally utilized in the clinical practice to analysis of the treatment plans. However, insight into the DVH curve with the application of the radiobiological analysis may be more critical in accessing the extensive quality of the radiotherapy treatment plans.[31,32] Many studies have suggested that radiobiological modeling that can instantly represent local tumor control and normal tissue complications is a key factor in choosing the optimal radiotherapy technique.[33-35]

To enhance the reliability of this analysis, two independent predicting models were utilized in this study. Interestingly, similar patterns in NTCP are found, and the findings of this analysis are further confirmed reliably. Collectively, this study strongly proposed that radiobiological evaluation should be routinely used in clinical practice to overcome the deficit of dosimetric analysis.

The main clinical motivation behind exploring advanced CSI treatment techniques represents the potential for the superior sparing of normal tissue. Various studies like Sharma *et al*.[14] compared CSI treatment for pediatric patients with 3DCRT, IMRT, and HT techniques. In contrast with the other strategies, the analysis concluded that HT was technically simpler and potentially dosimetrically beneficial. Seppala *et al*.[36] have found a means of fixing CSI target dose homogeneity with dynamic split-field IMRT technique. In a single-patient analysis, Penagaricano *et al*.[37] reported the dosimetric benefits of the tomotherapy plan compared with the 3DCRT plan. Kunos *et al*.[38] investigated the role of tomotherapy-based CSI in limiting dose to growing vertebral rings in four pediatric patients with medulloblastoma and compared it with conventional techniques.

There were different patterns in a study of PTV coverage and dose homogeneity for IMRT, VMAT, and HT. The target coverage and dose distributions for locally advanced esophageal cancer were compared by Wang *et al*.[39] with the simultaneous integrated boost technique of IMRT, VMAT, and HT. PBS was superior to VMAT and IMRT as far as the CI and HI were concerned. Howell *et al*.[40] compared the photon and proton CSI treatment dosimetrically and have established that the proton CSI improved normal tissue sparing while also providing more homogeneous target coverage than photon CSI at an equivalent time they need not taken into account the biological effectiveness.

This research showed outstanding target coverage with good dose homogeneity of 0.96 and favorable normal tissue sparing with PBS plan compared with other techniques. The highest CI was observed in the HT plan for the PTV brain. The drop in CI with the HT plan for PTV spine was noted, which may be due to the use of directional blocks in the region of kidneys, which pull the prescription isodose in the anteroposterior direction. The lung dose was observed lowest in the PBS plan and highest in the VMAT plan, followed by the 3DCRT plan. The results in these studies are incomparable directly with any of the previously published studies since none of them have compared the same data set to 3DCRT, IMRT, VMAT, and PBS techniques.

This study demonstrated that tomotherapy was a good option with less lung and heart doses with the excellent dose conformity and uniformity of the PTV. VMAT was relatively appropriate with less thoracic involvement. The dosimetric study was conducted by Zhang *et al*.[41] of IMRT, VMAT, TomoDirect (TD), and HT plans in upper thoracic esophageal cancer, which recorded that the HT plan was considered as an ideal choice with a wonderfully homogeneous and extremely conformal dose for PTV.

The increase in whole-body exposure and the higher volumes of normal tissues irradiated with relatively lower doses of radiation than traditional radiation is frequently the major concern in modern radiotherapies such as IMRT and VMAT, particularly in children. Both can potentially increase the secondary risk of malignancy caused by radiation, especially in children and long-term survivors. The dosimetric parameters and the probability of secondary cancer produced by proton beam therapy in scattering mode were compared by Yoon *et al*.[42] with the conventional RT and HT plans for pediatric CSI patients. Average doses of the proton therapy plan were lower for the chest and abdomen than for 3DCRT or Tomotherapy. Sakthivel *et al*.[43] accessed the risk of secondary malignant neoplasm in CSI for pediatric patients in PBS, HT, VMAT, IMRT, and 3DCRT using a mechanistic dose–response model that takes into account cell proliferation and mutation.

The limitations of this research will have to be discussed at this point. First, due to the small sample size study, several mitigating factors such as different planning systems and algorithms used for calculation could influence the results. In this study, the NTCP values have been estimated using radiobiological models, without adequate consideration of the tumor cell repopulation and oxygenation during the treatment course. The dose calculation algorithm and the radiobiological model are also the limitations of this study. Not all plans used the reference standard MC for calculation. The radiobiological parameters (D50, n, m, and α/β) that are used to compute the tissue responses are defined by large uncertainties.

Conclusion

The treatment plans can be ranked and compared with the NTCP estimated with a virtuous standardization for radiobiological parameters along with dosimetric parameters, which help the clinical practitioner or medical physicists to choose the best treatment plan for each patient based on their anatomical or clinical challenges. Good conformity and homogeneity were observed in HT and PBS plan for cranial and spinal fields, respectively. With respect to respiratory and renal complications, the PBS plan yields less complication than all other plans and the lung NTCP was higher in the VMAT plan. The 3DCRT plan shows the higher complication for optic structures compared to all other techniques. Moreover, the radiobiological parameters must be extensively used to select the treatment plan in the clinical practice at the same time. Weight loss of the patient must be carefully analyzed because modern radiotherapy techniques are dependent on the total volume involved in the treatment plan.

Financial support and sponsorship

Nil.

Conflicts of interest

There are no conflicts of interest.

References

1. Kirsch DJ, Tarbell NJ. Conformal radiation therapy for childhood CNS tumors. Oncologist2004;9:442-50.
2. Stacy W, Melva P, Daniel J, Allan F, Kenneth E. Clinical experience with radiation therapy in the management of neurofibromatosis-associated central nervous system tumor's. Int J Radiat Oncol Biol Phys 2009;73:208-13.
3. Daniel M, Kimberly M, Richard S. Medical and neurocognitive late effects among survivors of childhood central nervous system tumors. Am Cancer Soc 2001;92:10. [doi: 10.1002/1097-0142(20011115) 92:10<2709:AID-CNCR1625>3.0.CO; 2-D].
4. Mesbahi A, Rasouli N, Nasiri B. Radiobiological model-based comparison of three-dimensional conformal and intensity-modulated radiation therapy Plans for nasopharyngeal carcinoma. Iran J Med Phys 2017;14:190-6. [doi: 10.31661/JBPE.V9I3JUN.655].
5. Chatterjee S, Willis N, Locks SM, Mott JH, Kelly CG. Dosimetric and radiobiological comparison of helical tomotherapy, forward-planned intensity-modulated radiotherapy and two-phase conformal plans for radical radiotherapy treatment of head and neck squamous cell carcinomas. Br J Radiol 2011;84:1083-90.
6. Mesbahi A, Rasouli N, Mohammadzadeh M, Motlagh BN, Tekin HO. Comparison of radiobiological models for radiation therapy plans of prostate cancer: Three-dimensional conformal versus intensity modulated radiation therapy. J Biomed Phys Eng 2019;9:267-78.
7. Zaider M, Hanin L. Tumor control probability in radiation treatment. Med Phys 2011;38:574-83. [doi: 10.1118/1.3521406].
8. Lyman JT. Complication probability as assessed from dose-volume histograms. Radiat Res Suppl 1985;8:S13-9.
9. Marks LB, Yorke ED, Jackson A, Haken RK, Constine LS, Eisbruch A, *et al*. Use of normal tissue complication probability models in the clinic. Int J Radiat Oncol Biol Phys 2010;76:S10-9.
10. Niemierko A, Goitein M. Calculation of normal tissue complication probability and dose-volume histogram reduction schemes for tissues with a critical element architecture. Radiother Oncol 1991;20:166-76.
11. Halperin EC, Perez CA, Brady LW. "Perez and Brady's Principles and Practice of Radiation Oncology." 5th ed. Philadelphia: Wolters Kluwer

Health/Lippincott Williams and Wilkins; 2008.
12. Selek U, Zorlu F, Hurmuz P, Cengiz M, Turker A, Soylemezoglu F, *et al*. Craniospinal radiotherapy in adult medulloblastoma. Strahlenther Onkol 2007;183:236-40.
13. Athiyaman H, Mayilvaganan A, Singh D. A simple planning technique of craniospinal irradiation in the eclipse treatment planning system. J Med Phys 2014;39:251-8.
14. Sharma DS, Gupta T, Jalali R, Master Z, Phurailatpam RD, Sarin R. High-precision radiotherapy for craniospinal irradiation: Evaluation of three-dimensional conformal radiotherapy, intensity-modulated radiation therapy and helical tomotherapy. Br J Radiol 2009;82:1000-9.
15. Giantsoudi D, Seco J, Eaton BR, Simeone FJ, Kooy H, Yock TI, *et al*. Evaluating intensity modulated proton therapy relative to passive scattering Proton therapy for Increased Vertebral Column Sparing in CSI in Growing Pediatric Patients. Int J Radiat Oncol Biol Phys 2017;01:226.
16. Lyman JT, Wolbarst AB. Optimization of radiation therapy: A method of assessing complication probabilities from dose-volume histograms. Int J Radiat Oncol Biol Phys 1987;13:103-9.
17. Kutcher GJ, Burman C. Calculation of complication probability factors for non-uniform normal tissue irradiation: The effective volume method. Int J Radiat Oncol Biol Phys 1989;16:1623-30.
18. Kutcher G, Burman C, Brewster L, Goitein M, Mohan R. Histogram reduction method for calculating complication probabilities for three-dimensional treatment planning evaluations. Int J Radiat Oncol Biol Phys 1991;21:137-46.
19. Emami B, Lyman J, Brown A, Coia L, Goitein M, Munzenrider JE, *et al*. Tolerance of normal tissue to therapeutic irradiation. Int J Radiat Oncol Biol Phys 1991;21:109-22.
20. Gay HA, Niemierko A. A free program for calculating EUD-based NTCP and TCP in external beam radiotherapy. Phys Med 2007;23:115-25.
21. Niemierko A. A generalized concept of equivalent uniform dose (EUD). Med Phys 1999;26:1100.
22. Sohn M, Yan D, Liang J, Meldolesi E, Vargas C, Alber M. The incidence of late rectal bleeding in high-dose conformal radiotherapy of prostate cancer using EUD-and dose-volume based NTCP models. Int J Radiat Oncol Biol Phys 2007;67:1066.
23. Sanchez-Nieto B, Nahum AE. Bioplan: Software for the biological evaluation of radiotherapy treatment plans, Med Dosim 2000;25:71-6.
24. Bauman G, Yartsev S, Coad T, Fisher B, Kron T. Helical tomotherapy for craniospinal radiation. Br J Radiol 2005;78:548-52.
25. Schwarz M, Pierelli A, Fiorino C, Fellin F, Cattaneo GM, Cozzarini C, I. Helical tomotherapy and intensity modulated proton therapy in the treatment of early stage prostate cancer: A treatment planning comparison. Radiat Oncol 2011;98:74-80.
26. Widesott L, Pierelli A, Fiorino C, Dell'oca I, Broggi S, Cattaneo GM, *et al*. Intensity-modulated proton therapy versus helical tomotherapy in nasopharynx cancer: Planning comparison and NTCP evaluation. Int J Radiat Oncol Biol Phys 2008;72:589-96.
27. Brenner DJ. The linear-quadratic model is an appropriate methodology for determining isoeffective doses at large doses per fraction. Semin Radiat Oncol 2008;18:234-9.
28. Stavreva N, Nahum A, Markov K, Ruggieri R, Stavrev P. Analytical investigation of the possibility of parameter invariant TCP-based radiation therapy plan ranking. Acta Oncologica 2010;49:1324-33.
29. Warkentin B, Stavrev P, Stavreva N, Field C, Fallone BG. A TCP-NTCP estimation module using DVHs and known radiobiological models and parameter sets. J App Med Phys 2004;5:50-63.
30. Santiago A, Barczyk S, Jelen U, Engenhart-Cabillic R, Wittig A. Challenges in radiobiological modeling: Can we decide between LQ and LQ-L models based on reviewed clinical NSCLC treatment outcome data? Radiat Oncol 2016;11:67.
31. Oinam AS, Singh L, Shukla A, Ghoshal S, Kapoor R, Sharma SC. Dose volume histogram analysis and comparison of different radiobiological models using in-house developed software. Med Phys 2011;36:220-9.
32. Mesbahi A, Oladghaffari M. An overview on the clinical application of radiobiological modeling in radiation therapy of cancer. Int J Radiol Radiat Ther 2017;2:9-14. [doi: 10.15406/ijrrt. 2017.02.00013].
33. Sakthivel V, Kadirampatti Mani G, Mani S, Boopathy R, Selvaraj J. Estimating Second Malignancy Risk in Intensity-Modulated Radiotherapy and Volumetric-Modulated Arc Therapy using a Mechanistic Radiobiological Model in Radiotherapy for Carcinoma of Left Breast. J Med Phys 2017;42:234-40.
34. Widesott L, Pierelli A, Fiorino C, Lomax AJ, Amichetti M, Cozzarini C, *et al*. Helical tomotherapy vs. intensity-modulated proton therapy for whole pelvis irradiation in high-risk prostate cancer patients: Dosimetric, normal tissue complication probability, and generalized equivalent uniform dose analysis. Int J Radiat Oncol Biol Phys 2011;80:1589-600.
35. Rana S, Cheng C, Zhao L, Park SY, Larson G, Vargas C, *et al*. Dosimetric and radiobiological impact of intensity modulated proton therapy and RapidArc planning for high-risk prostate cancer with seminal vesicles. J Med Radiat Sci 2016;64:18-24.
36. Seppala J, Kulmala J, Paula L, Minn H. A method to improve target dose homogeneity of craniospinal irradiation using dynamic split field IMRT. Radiother Oncol 2010;96:209-15.
37. Penagaricano J, Moros E, Peter C, Saylors R, Ratanatnarathorn V. Paediatric craniospinal axis irradiation with helical tomotherapy: Patient out come and lack of acute pulmonary toxicity. Int J Radiat Oncol Biol Phys 2009;75:1155-61.
38. Kunos CA, Dobbins DC, Kulasekere R, Latimer B, Kinsella TJ. Comparison of helical tomotherapy versus conventional radiation to deliver craniospinal radiation. Technol Cancer Res Treat 2008;7:227-33.
39. Wang L, Li C, Meng X, Li C, Sun X, Shang D, *et al*. Dosimetric and radiobiological comparison of external beam radiotherapy using simultaneous integrated boost technique for esophageal cancer in different location. Front Oncol 2019;9:674.
40. Howell M, Giebeler A, Koontz R., Comparison of therapeutic dosimetric data from passively scattered proton and photon craniospinal irradiations for medulloblastoma. Radiat Oncol 2012;7:116. [doi: 10.1186/1748-717X-7-116.
41. Zhang Y, Wang H, Huang X, Zhang Q, Ren R, Sun R, *et al*. Dosimetric comparison of TomoDirect, helical tomotherapy, VMAT, and ff-IMRT for upper thoracic esophageal carcinoma. Med Dosim 2019;44:167-72.
42. Yoon M, Shin DH, Kim J, Kim DW, Park SY, Lee SB, *et al*. Craniospinal irradiation techniques: A dosimetric comparison of proton beams with standard and advanced photon radiotherapy. Int J Radiat Oncol Biol Phys 2011;81;637-46.
43. Sakthivel V, Ganesh M, McKenzie C, Boopathy R, Selvaraj J. Second malignant neoplasm risk after craniospinal irradiation in X-ray-based techniques compared to proton therapy. Australas Phys Eng Sci Med 2019;42:201-9.